كلية الهندسة بشبرا
FACULTY OF ENGINEERING AT SHOUBRA
ERJ
ISSN:1687-1340

ENGINEERING RESEARCH JOURNAL (ERJ)
Volume (52),Issue (1)
January 2023, pp:101-108
https://erjsh.journals.ekb.eg

Verification of Numerical Modelling of Tunnel-Shaft Connection under Static Loading

Mahmoud S. Nafi[1,*], Nasser M. Saleh[2], Nisreen E. Elfaris[3], Waleed A. Dawoud[4]

[1] *National Authority for Tunnels*
[2] *Geotechnical Engineering Department of civil engineering, Faculty of Engineering at Shoubra, Benha University, Cairo, Egypt.*
[3] *National Authority for Tunnels*
[4] *Geotechnical Engineering Department of civil engineering, Faculty of Engineering at Shoubra, Benha University, Cairo, Egypt.*
**Corresponding author*

E-mail address: mahmoud.s.nafi@gmail.com, na_sa_64@hotmail.com, yasmina_bosy@yahoo.com, walid.dawoud@feng.bu.edu.eg

Abstract: Needless to say, tunnels and shafts are versatile structures that are used for solving many problems all over the world. In this paper, verification was done for a finite element model for the connection between tunnel and shaft under static loading using Midas GTS NX software. Tunnel-shaft connection 17A between Kolleyet El-Banat and Al-Ahram stations, from Greater Cairo Metro Line 3, Phase 2, was used as the case study of this paper. Full details of FEM model inputs were introduced and stages of construction were mentioned. Results from the model were verified using settlement monitoring results. After that, settlement results from the model were also discussed to highlight the effect of executed works. The provided verified model can be further used for analyzing more outputs and for making sensitivity analysis or parametric study on such problems.

Keywords: Tunnel, Shaft, Connection, Greater Cairo Metro, FEM

1. Introduction

The problem of population growth all over the world creates a persistent need to escape with the transportation process from the over ground to the underground. Tunnels are versatile underground passageways that may be used for that purpose. Nowadays, many countries are depending on tunnels to solve their problems with the transportation process. For that reason, the world is witnessing a great leap in the technology of design and construction of tunnels.[1][2]

Underground space use has been cared for throughout history and has become indispensable to be employed nowadays. The first railway underground metro was constructed in London and opened in 1863 as per [3], and since then the culture of underground railway systems has increased and distributed all over the world, and of course in Egypt. Egypt has a very old history of employing underground space since the Pharaohs as per [4], and it was the first country to have a metro line in Africa, Cairo Metro Line 1, in the 80s, as per [5].

Shafts are vertical openings that are usually used as annexed structures to tunnels for some safety issues. Shafts are used especially for long tunnels as an economical natural ventilation system and an emergency egress. They are also used as entrances to the tunnel working face to accelerate the construction process. The intersection between tunnels and shafts is a challenging construction issue. This 3-dimensional problem needs a thorough knowledge of the geological and geotechnical conditions of surrounding soil so as to be properly studied.[6][7]

Greater Cairo Metro is a huge project that commenced in the 1980s. It was an alternative solution to the problem of traffic congestion in Greater Cairo whose population reached some millions. Line 3 of Greater Cairo is extended from Cairo Airport on the east to Imbaba and Cairo University on the west. It consists of a group of stations of various types, i.e.: underground, at grade, and elevated stations. For safety and ventilation issues, the tunnel between any two consecutive underground stations is chosen to be intersected with a vertical shaft. One of those shafts will be chosen the be the main scope of the research.[8]

In recent years, many researchers have employed numerous numerical methods to analyze such problems. Of those methods, the finite difference method (FDM) and finite element method (FEM) have been the most to be touched upon by researchers. These methods have been widely used to get the stress distributions and deformation patterns of tunnels generically and intersections specifically.[9]

[10] studied the effect of tunneling at shallow depths using TBM on surrounding structures, with a case study of the Greater Cairo Metro. They used 3D finite element and considered many processes that affect tunneling, such as face pressure, shield overcutting, etc. They employed two constitutive models, Double Hardening Soil Model (DHS-Model) and the Hardening Soil Model under Small Strains (HSSS-Model), and compared the results with field monitoring. They stated that HSSS-model settlement results show a better agreement with the field than DHS-model.

[11] executed an experimental study to evaluate the structural response of segmental tunnel linings, with steel fibers reinforcement under real-life loading in hard ground conditions. They designed an in-situ real-scale test for a real

segmental tunnel and applied it at a part of the new Line 9 (L9) of the metro of Barcelona. This study was also beneficial as it also considered the real ground-tunnel interaction, and studied also the feasibility of using steel fibers for tunnel segments. One of the conclusions was that stress distribution and structural response of tunnel rings depend highly on tangential ground-structure interaction, and the best approach is to make tangential stiffness equal to 1/3 of the radial stiffness for the lining.

[12] proposed a new model of loading with FEM analysis to investigate the behavior of shallow tunnels (cover-to-diameter ratio C/D< 2) in soft soils. They discussed internal forces and deformations for various shallow tunnels and the relation between the optimal thickness-to-diameter ratio d/D of the tunnel cross-section and the cover-to-diameter ratio C/D. They used The Second Heinenoord Tunnel in the Netherlands as a case study and compared the results of their model with field data and results from other researchers' works. It was found that the thinner the tunnel is (the less d/D ratio) and/or the larger the tunnel radius is, the higher the maximum radial displacement will be. Also, they found an optimal value for the C/D ratio that corresponds to minimum radial displacement, for various radii, with and without buoyancy.

[13] studied the construction stability of a cross passage and a shaft under two proposed construction methods: the "shaft followed by cross passage construction" method and the "cross passage parallel shaft construction" method. They used a numerical simulation and field measurements to compare between the two construction methods. The study area is a part of Subway Line 5 in Xi'an, China, and it was constructed through a layer of loess soil. Results showed that there is nearly no difference between the two construction methods, for ground surface settlement and plastic deformation, however, the location of maximum plastic deformation is only different. Regarding the results of displacement and stress of shaft structure, results showed that method 2 of construction, is better in controlling the displacement and stress of shaft, especially in the direction of excavation of cross-passage. The concentration of stresses for the two methods occurs near the horsehead of the cross passage near the connection, so this position needs special care than other locations, and to be the main spot to be reinforced while construction.

[14] investigated stress distributions and ground deformations around a tunnel intersection using a 3D finite element analysis for a case study- Hakim tunnel project, Tehran, Iran. The intersection of the parent and the child tunnels was intersected at an angle of 90°, and the new Austrian tunneling method (NATM), was selected as the method of excavation of both tunnels. Abaqus FEM software was used for the analysis of this problem and recorded data for the deformation of tunnel walls for parent and child tunnels were used to validate the model. They concluded that plastic zones and the bending moment were found to increase at main tunnel walls at the intersection, and axial force was found to increase at tunnel lining, due to executing intersection. The increase in axial force near the intersection can reach a value of 150%.

[15] discussed the structural response of a parent tunnel with a perpendicular child tunnel through an opening. They made a sensitivity analysis and compare between analytical solution, 2D and 3D Finite Element Analysis results, to use as a guide for the design and construction of tunnels' openings and intersections. Results showed that many parameters affect the stress redistribution around the opening, such as tunnel depth, child-to-parent tunnel diameters ratio, Young's model for soil, and confinement conditions around the tunnel. Also, 2D analysis is preferred over analytical solutions, and it was found that the opening shape affects the results of the 2D analysis. Besides, 3D analysis results showed that the opening size and soil stiffness have a great effect on stress distribution around the opening.

[16] discussed the deformations and stress distributions of a tunnel intersection with a subway station in China. They performed a 3D numerical analysis using Midas-GTS software, and results of deformations, stress responses, and plastic zones of rock mass and tunnel at the intersection zone were obtained. Also, the possible failure modes for tunnel linings were discussed. Authors stated that executing the intersection increases the deformation of the subway tunnels near the intersection, destroyed the stress path of the subway tunnel, and the stress deflected again to meet equilibrium. Also, plastic zones results showed a concentration of plastic zones at the intersection, especially at the sidewalls, so the rock around the intersection is more likely to be failed, so they recommended that the strength of rock around the intersection should be ensured to guarantee its stability during construction.

2. Numerical Modeling

2.1 Analysis planning

The main objective of this study is to assess the behavior of the connection between the tunnel and shaft under static loading and make a parametric study for different conditions to benefit from results in ongoing projects and future ones. The connection between the tunnel and Shaft 17A between Kolleyet El-Banat and Al-Ahram stations, Line 3 Phase 2, was chosen to be studied. Data from National Authority for Tunnels (NAT) was obtained to use for numerical modeling of the tunnel-shaft connection.

As per the method of construction in Line 3, the vertical shaft is constructed firstly using an earth retaining technique such as diaphragm walls. Later on, the tunnel was advanced using a Tunneling Boring Machine (TBM) until reaching the shaft. Then TBM breaks the connection between the tunnel and shaft to make the emergency and ventilation exit. From the design perspective, this connection maybe a weak point when exposed to static loads.

Midas GTS NX 2019 package was used for implementing the numerical simulation of our problem. GTS NX is a simulation program developed for the evaluation of soil-structure interaction based on the finite element method. GTS NX helps engineers to perform step-by-step analyses of excavation, structure placement,

loading, and other factors that directly affect design and construction. The program supports various conditions (soil characteristics, water level, etc.) and analytical methodologies to simulate real phenomena.[17]

2.2 Geometry modeling

2.2.1 Soil Layers

As per the geotechnical interpretative report for the tunnel from Kolleyet El Banat station to Al Ahram station, the stratigraphy and design parameters of soil at annex 17A zone are shown in Table 1. Below the thin clay layer, a continuous layer of dense sand is considered according to results from other boreholes. To correspond with the top level of constructed shaft, the model surface level is considered to be +50.48, and the fill layer is extended instead from +50.48 to +47.6 levels. The full model shows the stratigraphy of soil layers, tunnel, and shaft shown in Fig. 1.

TABLE 1. Stratigraphy of soil layers

Stratum	Average Level Range	Depth below ground level (m)
Man Made Fill	+50.1 to +47.6	+0.0 to +2.5
Upper Sand	+47.6 to +37.6	+2.5 to +12.5
Middle Sand	+37.6 to +29.5	+12.5 to +20.6
Upper Clay	+29.5 to +28.0	+20.6 to +22.1
Middle Sand	+28.0 to +17.8	+22.1 to +32.3
Lower Clay	+17.8 to +14.8	+32.3 to +36.8
Lower Sand	+14.8 to -4.00	+36.8 to +55.6

2.2.2 Tunnel

The tunnel is constructed using TBM, but for simplicity, the simulation of TBM movement wasn't taken into consideration. Only boundary condition by preventing the movement in (-Y) direction, was applied at the working face to guarantee the stability of the working face. The tunnel was simulated as if it was constructed through 3 phases, the tunnel before connection, the tunnel at connection, and the tunnel after connection. For the sake of more accurate results, the tunnel at the connection part was split into 12 rings, centered about the connection center, and each ring was 1.5 m in width. The whole tunnel linings simulated in the model are shown in Fig. 2, and the geometry parameters of tunnel linings used in the model are shown in Table 2.

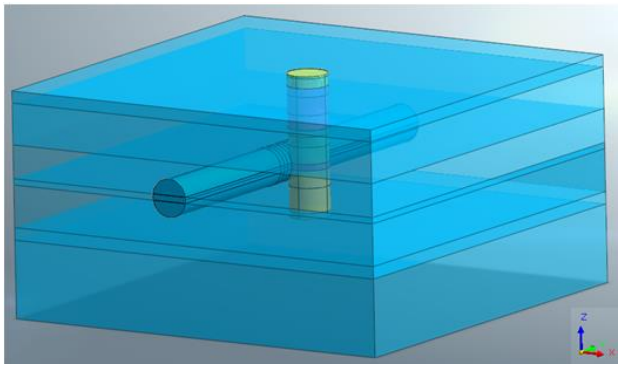

Fig. Full geometry for Midas model

Table2. Geometry parameters of tunnel linings

Parameter	Value
Thickness	0.4 m
Ring width	1.5 m
Center-to-center diameter	9.15 m

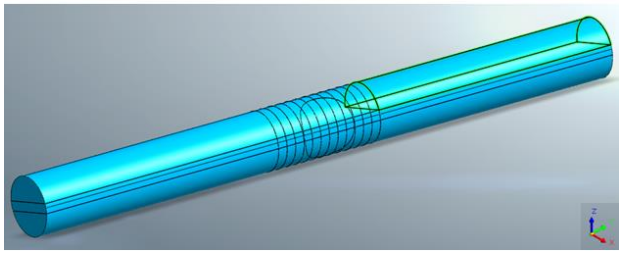

Fig2. Geometry of tunnel linings as simulated in Midas model

2.2.3 Shaft

The shaft was constructed with panels of diaphragm walls, with a center-to-center diameter of 9.665 m. It was simulated with geometry parameters shown in Table 3, and the as-simulated shaft is shown in Fig. 3.

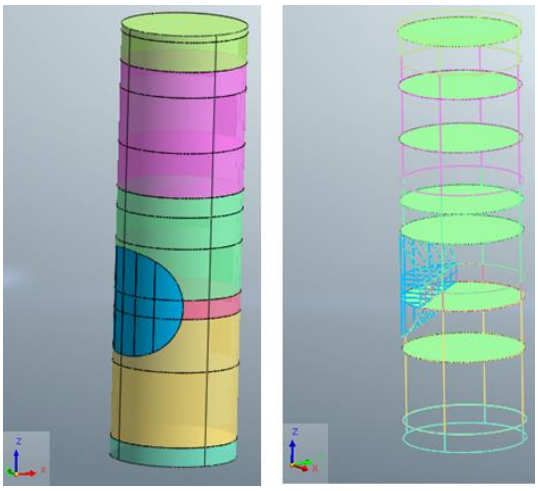

Fig3. Geometry of shaft and internal slabs as simulated in Midas model

Table3. Geometry parameters of shaft diaphragm walls

Parameter	Value
Thickness	0.8 m
Height	34.18 m
Center-to-center diameter	9.665 m

2.2.4 Internal Slabs

All underground internal slabs have a thickness of 0.25 m except the roof, 4th, and 5th underground slabs which have a thickness of 0.40 m. The Raft slab only has a thickness of 0.6 m. The levels and thicknesses of all internal slabs are shown in Table 4, and Fig. 3 shows internal slabs as simulated in Midas model.

Table4. Levels and thicknesses of internal slabs

Slab	Level	Thickness (m)
Roof Slab	+49.95	0.4
1st Slab	+45.55	0.25
2nd Slab	+41.15	0.25
3rd Slab	+36.05	0.25
4th Slab	+33.55	0.4
5th Slab	+27.97	0.4
Raft	+23.77	0.6

2.2.5 Tunnel-Shaft Connection

The distance between the shaft axis and tunnel axis is 6.60 m. Shaft diaphragm walls intersected tunnel linings in just 6 rings. Only a 6 m opening was executed which is equivalent to breaking only 4 out of 6 rings. The average height of the opening is 5.275 m, and it extended from the 5th internal slab to the top of the connection. The tunnel-shaft connection is shown in Fig. 4.

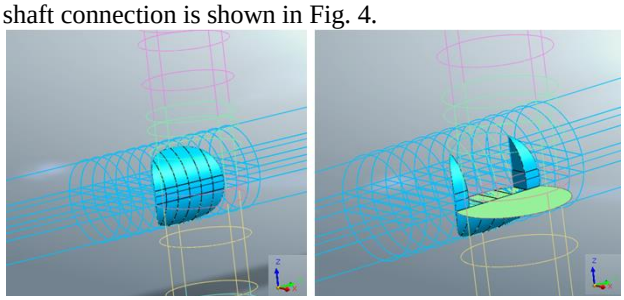

Fig 4. Tunnel-shaft connection geometry as simulated in Midas model

2.3 Meshing (Discretization)

The 3D model was considered for solving tunnel-shaft connection. Tetrahedron mesh type is chosen to represent the whole model. For mesh sizes, linear gradient was used to generate the mesh from center sized 1 m, to outside sized 4 m. All tunnel and shaft meshes, soil, or structure, have 1 m length in each direction. Figure 5 presents the mesh discretization of the model.

2.4 Defining material properties

Material properties required for constitutive models were got from soil interpretative reports. The following sections show tables of properties of all materials in the model.

2.4.1 Soil Layers

Table 5 presents the properties of soil layers, as obtained from geotechnical interpretative report.

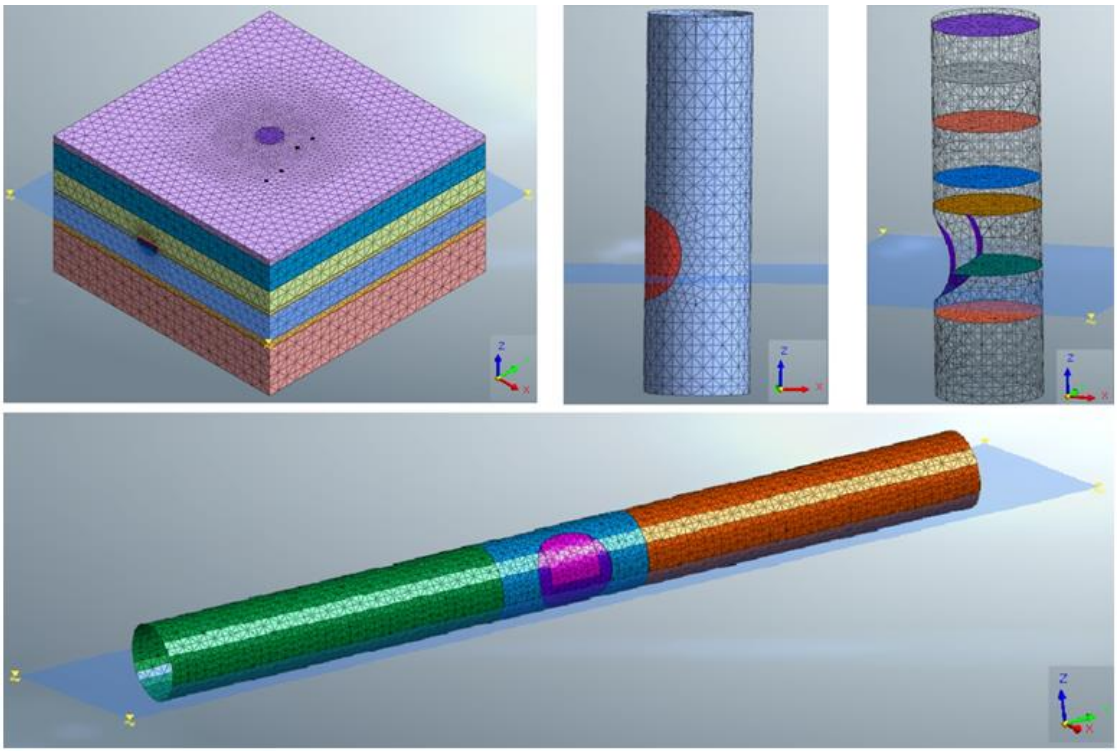

Fig 5.Meshes as represented in Midas mode

Table5. Material properties for soil layers

Stratum	γb (kN/m3)	C (kPa)	Φ (°)	K0	E (MPa)	ν
Man Made Fill	18	0.2	30	0.5	10	0.3
Upper Sand	19.5	0.2	37	0.4	70	0.3
Middle Sand	20	0.2	39	0.37	130	0.3
Lower Sand	21	0.2	40	0.36	150	0.3
Upper Clay	18	20	29	0.61	54	0.35
Lower Clay	19	30	27	0.66	59	0.35

2.4.2 Tunnel

Table 6 presents the physical properties of tunnel linings, as obtained from calculation notes, provided by National authority for Tunnels.

Table6.Material properties for tunnel linings

Parameter	Value
Specific self-weight	25 kN/m3
Long-term modulus of elasticity	Ec = 15.160 GPa
Poisson ratio	0.20

2.4.3 Shaft

Table 7 presents the physical properties of shaft diaphragm walls, as obtained from calculation notes, provided by National authority for Tunnels.

Table7. Material properties for shaft diaphragm walls

Parameter	Value
Specific self-weight	22 kN/m3
Long-term modulus of elasticity	Ec = 9.953 GPa
Poisson ratio	0.20

2.4.4 Internal Slabs

Table 8 presents the physical properties of shaft internal slabs, as obtained from calculation notes, provided by National authority for Tunnels.

Table8. Material properties for internal slabs

Parameter	Value
Specific self-weight	24 kN/m3
Long-term modulus of elasticity	Ec = 11.641 GPa
Poisson ratio	0.20

Solid continuum material is used for simulating all soil elements in the model. For other structure elements, tunnel, shaft and internal slabs, shell elements are used.[18]

2.5 Choosing the constitutive model

For the purpose of research, Mohr-Coulomb (MC) model was used to simulate the behavior of soil layers. The properties used for each layer were obtained from the ground interpretative report and each layer was simulated as a solid element. On the other side, all structure elements, tunnel segments, shaft diaphragm walls and internal slabs, were simulated as shell elements using the Isotropic Elastic model.[18]

2.6 Loads and boundary conditions

Only static load is considered in this analysis. This static load includes the self-weight of soil layers and a surcharge of 20 kN/m2 which represented buildings' weights at the surface.

As per [19], the horizontal boundaries to be (4:6) D, where D is tunnel diameter, and vertical boundaries to be (3:4) D. The full model has dimensions of 100 m×100 m×54.5 m, length, width, and depth accordingly. The distances around the tunnel-shaft connection were chosen to reduce boundary effects on results as per [19]. Boundary conditions are chosen to prevent movement in X and Y directions and permit movement in Z direction for all sides while preventing movement in all directions for the bottom side only.

2.7 Defining analysis stages

Generally, the construction stages are arranged and analyzed as follows:

1- Initial stage: which includes the full stratigraphy of soil and groundwater table and boundary conditions were applied. Also, the soil weight was activated and the surcharge which is equivalent to buildings weights at the surface was added.
2- D-wall installation: only the diaphragm walls of the shaft were executed.
3- Tunnel before connection: the first part of the tunnel was executed and soil was excavated. Also, boundary condition was applied at the tunnel working face to prevent the collapse of soil at the working face.
4- Tunnel at connection: the middle part of the tunnel was executed; the soil was excavated and the part of the shaft diaphragm walls inside the tunnel was demolished. As previously, a boundary condition was applied at the tunnel working face.
5- Tunnel after connection: the last part of the tunnel was executed and the remaining soil was excavated.
6- Excavation to top of connection: three soil layers were excavated out of the shaft, to reach a little above the top of the shaft-tunnel connection.
7- Excavation to the raft: other three layers were excavated out of the shaft to reach raft slab level. Also, the groundwater level is lowered to be 0.5m below the raft slab level.
8- Install raft slab: raft slab was executed and the groundwater level was risen and reached just below the raft slab.

9- Install 5th slab: 5th underground slab was executed, which is at the bottom level of broken segments.
10- Break the connection: 6m wide of tunnel segments inside shafts, 4segments, were broken; to open the connection between shaft and tunnel.
11- Install 4th slab: 4th underground slab was executed.
12- Install 3rd slab: 3rd underground slab was executed.
13- Install remaining slabs: other slabs until roof slab were executed in just one stage.

3. Model Verification and Discussion

The surface settlement obtained from the numerical results at stage 6, is compared with the monitored settlement at Elevation Reference Points (ERPs), measured at the same stage. Four points were selected for comparison that represent four corners for two different buildings beside the shaft, as shown in Fig. 6a. The good agreement between the numerical results and the field measured values is clearly depicted in Fig 6b.

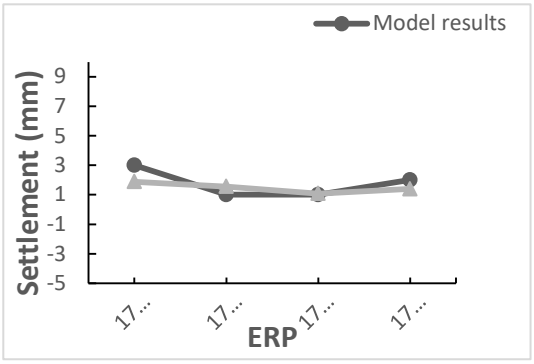

(a)

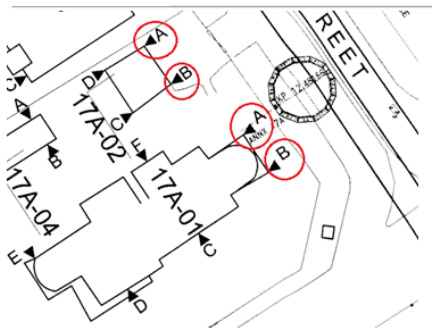

(b)

Fig 6.(a) Location of ERP points, **(b)** Model verification

The obtained numerical settlements at Ground Level (GL) and around connection will be discussed in the following two sections.

3.1 Settlement at GL

Generally, the maximum settlement at the ground surface occurs directly above the tunnel, and is increasing with the advancing of the tunnel, as shown in Fig. 7a. After completing tunnel excavation, a higher value of heave is observed, next to the shaft; due to excavation works inside the shaft. This heave reaches its maximum value in stage 8 when the raft level is reached, as depicted inFig.7b.

Also, Fig. 8 shows the settlement of three points at GL, one directly above the tunnel center, referred as (PC), and the two other points are chosen to the right and left of it in such a manner that, and the lines connecting between them and the tunnel center making 45° angles with the vertical line through the tunnel center, and referred as (PR) and (PL) respectively. Settlement rough at the stage with the max settlement is also provided in Fig. 9. The three curves in the figure reveal that:

1- The point (PC), directly above the tunnel axis shows the max settlement between the three points, which was clearly expected; due to its proximity to tunnel excavation. Also, values of settlement may be different from actual; as TBM excavation and uplift pressure weren't fully simulated, that may be covered in future studies.

2- The settlement at the three points increases due to shaft diaphragm wall installation and decreases through all tunnel excavation stages, then they experience heave since the start of excavation inside the shaft and becomes nearly constant for the remaining activities.

3- Breaking the connection between the tunnel and shaft seems to have no effect on changing settlement or heave values.

4- The settlement rough at the stage with maximum settlement value shown in Fig. 9 also reveals the same remarks as above

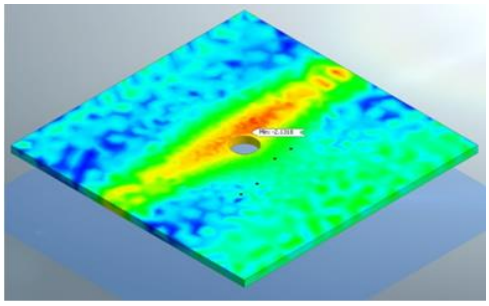

(a)

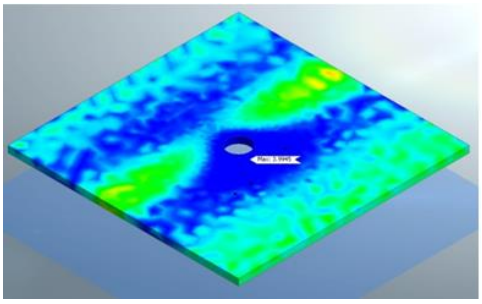

(b)

Fig 7.(a) Maximum surface settlement above the tunnel in stage 5, **(b)** Maximum heave next to the shaft in stage 8

3.2 Settlement around the connection

Three points were selected; to track settlement around the connection, point C1 at the tunnel perimeter, point C2 is around 2.7 m above, and point C3 is around 4.25 m above, as shown in Fig. 10. The resulted settlements at the selected locations are depicted in Fig. 11, where it was found that:

1- Variation of settlements showed some similarity to settlement at GL, that settlement increases due to shaft diaphragm wall installation, but showed a higher settlement in stage 4, tunnel at connection, and they experienced heave since the start of excavation inside the shaft and becomes nearly constant for the remaining activities.

2- Also, Breaking the connection between the tunnel and shaft seems to have no effect on changing settlement or heave values.

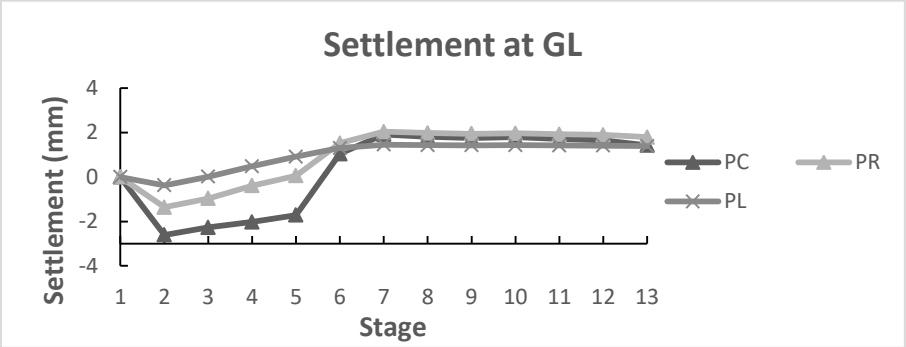

Fig 8. Variation of settlement at GL

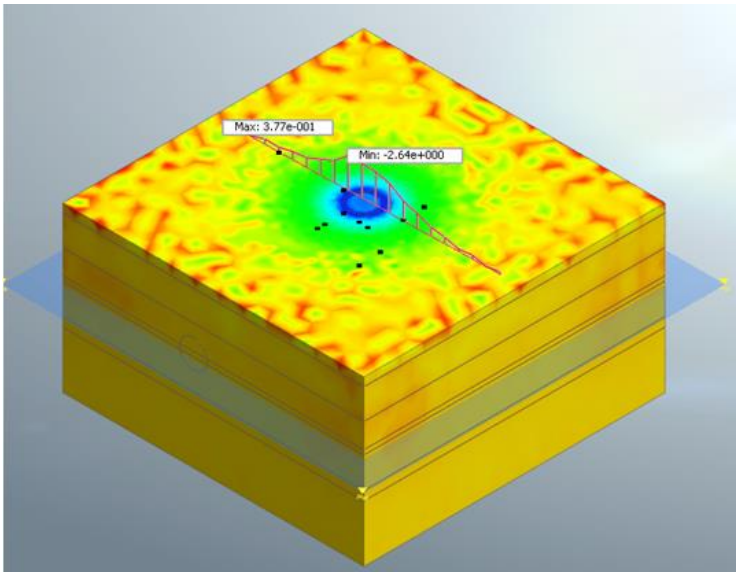

Fig 9. Settlement rough at the stage with maximum settlement value

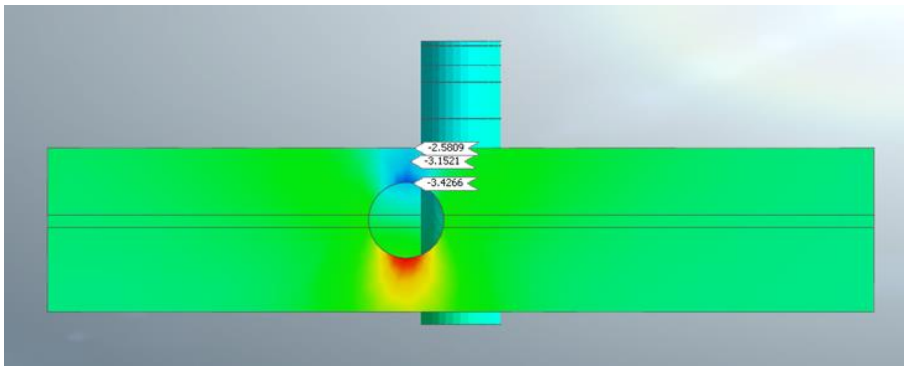

Fig 10.Maximum settlement at chosen nodes around the connection

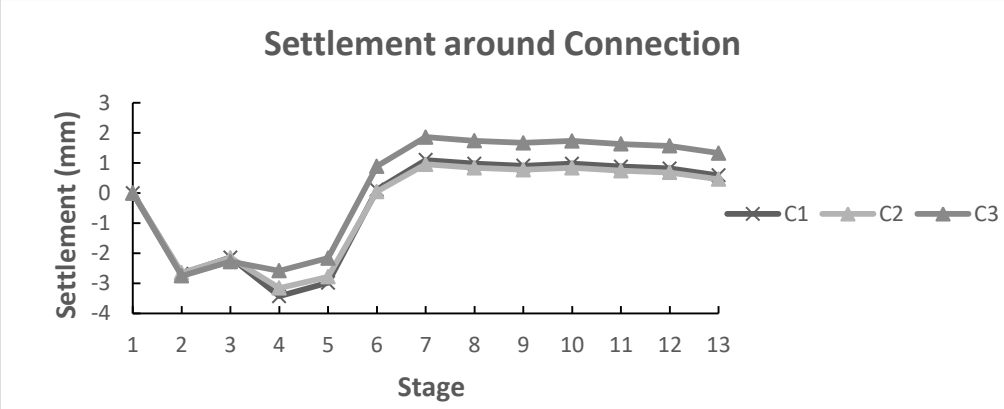

Fig 11. Variation of settlement around the connection

4. CONCLUSIONS

From the current study, some conclusions can be presented as follows:

1. FEM numerical models are considerable when simulating tunnel-shaft problems.
2. Tunnel-shaft connection problems are 3D problems, which are affected by many parameters.
3. Settlement at ground level is affected by diaphragm wall installation and tunnel advancing, and it shows heave for the stages of work inside the shaft, but breaking the connection between tunnel and shaft shows no effect on settlement and heave values.
4. Settlement near the connection has the maximum value when tunneling at the connection zone, and except for that, it has a similar trend to settlement at GL.
5. The tunnel-shaft connection must be cared for in the design and construction process, and be the focus of more studies.

REFERENCES

[1] Lane, K. S. (2019). Tunnels and underground excavations. In Encyclopædia Britannica. Retrieved from https://www.britannica.com/technology/tunnel.

[2] Alielahi, H., &Adampira, M. (2016). Effect of twin-parallel tunnels on seismic ground response due to vertically in-plane waves. International Journal of Rock Mechanics and Mining Sciences, 85, 67–83.

[3] Cui, J., & Nelson, J. D. (2019). Underground transport: An overview. 87(December 2018), 122–126. https://doi.org/10.1016/j.tust.2019.01.003.

[4] EL Salam, M. E. A. (2002). Construction of underground works and tunnels in ancient Egypt.Tunnelling and Underground Space Technology, 17(April 2001), 295–304.

[5] Patrizi, P. (2012). The Line 3 of the Metro of Cairo.Geotechnical Aspects of Underground Construction in Soft Ground – Viggiani (Ed), 239–246.

[6] Wang, T. T., Lee, T. T., Lee, S. M., Li, K. S., & Chen, C. H. (2016). Tunneling issues regarding the rock tunnel-shaft intersection in Taiwan. Geotechnical Engineering, 47(2), 14–23.

[7] Ji, J., Han, J. Y., Fan, C. G., Gao, Z. H., & Sun, J. H. (2013). Influence of cross-sectional area and aspect ratio of shaft on natural ventilation in urban road tunnel. International Journal of Heat and Mass Transfer, 67, 420–431.

[8] Systra. (2014). Greater Cairo Metro Al Thawra Line (Line 3)-Phase 3, Tender Document, Underground Section, Civil Works Specifications.

[9] Li, Y., Jin, X., Lv, Z., Dong, J., &Guo, J. (2016). Deformation and mechanical characteristics of tunnel lining in tunnel intersection between subway station tunnel and construction tunnel. Tunnelling and Underground Space Technology, 56, 22–33. https://doi.org/10.1016/j.tust.2016.02.016.

[10] El-Nahhas, F.M.; El-Mossalamy, Y. M.; and El-Shamy, A. A. (2015). 3D Analysis of Ground Settlement Induced By Mechanized Tunnelling.Fourteenth Int. Conference on Structural and Geotechnical Eng. (ICSGE 14).

[11] Molins, C., &Arnau, O. (2011). Experimental and analytical study of the structural response of segmental tunnel linings based on an in situ loading test. Part 1: Test configuration and execution. Tunnelling and Underground Space Technology, 26(6), 764–777. https://doi.org/10.1016/j.tust.2011.05.002.

[12] Ngan Vu, M., Broere, W., & Bosch, J. W. (2017).Structural Analysis for Shallow Tunnels in Soft Soils.International Journal of Geomechanics, 17(8), 04017038.https://doi.org/10.1061/(asce)gm.1943-5622.0000866.

[13] Song, Z., Cao, Z., Wang, J., Wei, S., Hu, S., &Niu, Z. (2018). Optimal Analysis of Tunnel Construction Methods through Cross Passage from Subway Shaft.Advances in Civil Engineering, 2018, 1–14. https://doi.org/10.1155/2018/5181954.

[14] Joneidi, M., Golshani, A., &Naeimifar, I. (2019). Progressive deformation and mechanical behaviour of intersecting tunnels in soft ground.Proceedings of the Institution of Civil Engineers - Ground Improvement, 2017, 1–12. https://doi.org/10.1680/jgrim.18.00073.

[15] Spyridis, P., &Bergmeister, K. (2015). Analysis of lateral openings in tunnel linings.Tunnelling and Underground Space Technology, 50, 376–395. https://doi.org/10.1016/j.tust.2015.08.005.

[16] Li, Y., Jin, X., Lv, Z., Dong, J., &Guo, J. (2016). Deformation and mechanical characteristics of tunnel lining in tunnel intersection between subway station tunnel and construction tunnel. Tunnelling and Underground Space Technology, 56, 22–33. https://doi.org/10.1016/j.tust.2016.02.016.

[17] MIDAS Information Technology Co., Midas GTS NX 2019 v2.1, User Manual, Chapter 1: Introduction, 2019.

[18] MIDAS Information Technology Co., Midas GTS NX 2019 v2.1, User Manual, Chapter 4: Mesh, 2019.

[19] Lees, A. (2016). Geotechnical finite element analysis: a practical guide.